NANOSTRUCTURED MATERIALS

Grain size effect on deformation twinning and detwinning

Y. T. Zhu · X. Z. Liao · X. L. Wu · J. Narayan

Abstract This article systematically overviews the grain size effect on deformation twinning and detwinning in face-centered cubic (fcc) metals. With decreasing grain size, coarse-grained fcc metals become more difficult to deform by twinning, whereas nanocrystalline (nc) fcc metals first become easier to deform by twinning and then become more difficult, exhibiting an optimum grain size for twinning. The transition in twinning behavior from coarse-grained to nc fcc metals is caused by the change in deformation mechanisms. An analytical model based on observed deformation physics in nc metals, i.e., grain boundary emission of dislocations, provides an explanation of the observed optimum grain size for twinning in nc fcc metals. The detwinning process is caused by the interaction between dislocations and twin boundaries. Under a certain deformation condition, there exists a grain size range where the twinning process dominates over the detwinning process to produce the highest density of twins.

Introduction

Materials are usually either strong or ductile, but rarely both at the same time [1–6]. Deformation twinning is one of the few mechanisms that can increase both the strength and the ductility simultaneously [7–14]. Therefore, it is of interest to understand factors that affect the deformation twinning, including the microstructures, intrinsic physical properties, etc. It is well known that the activation of deformation twinning is affected significantly by deformation temperature [15–19], strain rate [15, 16, 19–23], and stacking fault energy [10, 15, 16, 24–33]. Recently, generalized planar fault energies [34–37] and grain size [38–47] were found to play significant roles in deformation twinning. In addition, detwinning was also found to be active during the deformation of materials that contain twins [48–50], and in some cases twinning and detwinning occur concurrently and compete with each other [48].

The grain size effect on twinning and detwinning is critically important for designing the microstructures of materials, especially nanocrystalline (nc) materials, for the best mechanical properties. It also affects the stability of nc materials under some service conditions such as cyclic loading. However, the knowledge on this topic is currently fragmented because it is a relatively new topic and has not been systematically overviewed before. Therefore, this article systematically overview the grain size effect on the twinning and detwinning of face-centered cubic (fcc) metals by examining experimental data and theories reported in the literature. The grain size effect in hcp and bcc metals will be only briefly discussed as they have not been studied well.

Y. T. Zhu (✉) · J. Narayan
Department of Materials Science and Engineering, North Carolina State University, Raleigh, NC 27695, USA
e-mail: ytzhu@ncsu.edu

Y. T. Zhu
School of Materials Science and Engineering, Nanjing University of Science and Technology, Nanjing, China

X. Z. Liao
School of Aerospace, Mechanical and Mechatronic Engineering, The University of Sydney, Sydney, NSW 2006, Australia

X. L. Wu
State Key Laboratory of Nonlinear Mechanics, Institute of Mechanics, Chinese Academy of Sciences, Beijing 100190, China

Experimental observations on the grain size effect

The grain size effect on deformation twinning was observed mostly by experimental observations, instead of being predicted by computer simulations. In this section, we present the experimental observations on the grain size effect for a broad grain size range from coarse grains (larger than 1 μm) to nanometer-sized grains (smaller than 100 nm), which can be schematically described in Fig. 1. In brief, in the coarse-grain size range, deformation twinning becomes more difficult with decreasing grain size for fcc, bcc, and hcp metals [17], whereas in the nc grain size range, with decreasing grain size twinning first becomes easier (the normal grain size effect) and then more difficult (the inverse grain size effect) [40, 42] in fcc metals and alloys. This results in an optimum grain size that is easiest to deform by twinning for fcc metals [40, 42]. However, the twining behavior in nc bcc and hcp metals have not been well studied, although it is generally observed that nc hcp metals are more difficult to twin than their coarse-grained counterparts. It should be noted that the critical grain size for the transitions in deformation twinning behavior may be affected by intrinsic material properties such as the stacking fault energy as well as external deformation conditions such as strain rate and deformation temperature.

Grain size effect on twinning in coarse-grained materials

It has been observed that larger grains are easier to deform by twinning for coarse-grained materials [17, 51]. This was explained as follows [17]. It is well known that the critical stress for dislocation slip can be described by the Hall–Petch relationship $\sigma_S = \sigma_0 + k_S\, d^{-1/2}$, where d is grain size, σ_0 is a constant, and k_S is the Hall–Petch slope for dislocation slip. Experimental results indicate that the critical stress for twinning also shows a Hall–Petch type

behavior, $\sigma_T = \sigma_{0'} + k_T\, d^{-1/2}$, where k_T is the Hall–Petch slope for twinning. Table 1 summarizes the Hall–Petch slopes for both dislocation slip and twinning for some fcc, bcc, and hcp metals. For coarse-grained fcc metals, it is obvious that k_T is larger than k_S, which means that with decreasing grain size the critical stress required for twinning increases faster than that for dislocation slip, as schematically illustrated in Fig. 2. In other words, twinning becomes more difficult than dislocation slip with decreasing grain size. The physical reason for such a grain size effect in coarse-grained metals is not understood. Yu et al. [52] recently attempted to explain such a phenomenon by a

Table 1 The Hall–Petch slopes for fcc, bcc, and hcp metals and alloys [17]

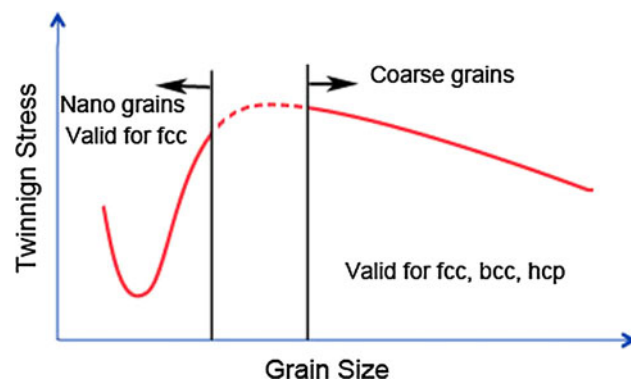| Material	k_S for dislocation slip (MPa mm$^{1/2}$)	k_T for twinning (MPa mm$^{1/2}$)	κ_T/κ_S
fcc			
Cu	5.4 (RT)	21.7 (77 K)	4
Cu–6 wt% Sn	7.1	11.8 (77 K), 7.9 (RT)	1.7, 1.1
Cu–9 wt% Sn	8.2	15.8 (77 K)	1.9
Cu–10 wt% Zn	7.1	11.8 (77 K)	1.7
Cu–15 wt% Zn	8.4	16.7 (295 K)	2.0
bcc			
Fe–3 wt% Si	12	100	8.3
Armco iron	20	124	6.2
Steel (1010, 1020, 1035)	20	124	6.2
Fe–25 at% Ni	33	100	3.0
Cr	10.1	67.8	6.7
V	3.5	22.4	6.4
hcp			
Zr	8.3	79.2	9.5
Ti	6	18	3.0

Fig. 1 Schematic description of grain size on the critical stress needed to activate deformation twinning. The grain size effect for nc bcc and hcp metals is uncertain
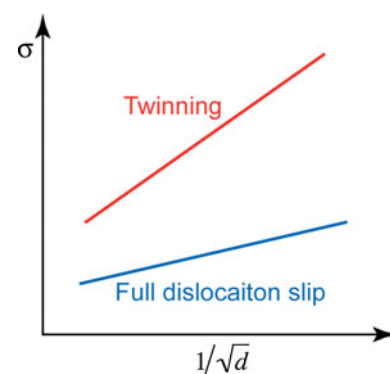

Fig. 2 The schematic of Hall–Petch relationship for twinning and full dislocation slip in coarse-grained metals and alloys. σ is the stress and d is the grain size [16]

"stimulated slip" mechanism. More studies are needed to probe its fundamental physics. It should be noted that these experimental observations are not consistent with the classical dislocation model [53, 54] that has been used to explain the grain size effect on twinning [31, 55].

Interestingly, the ratio of Hall–Petch slope for twinning to that for dislocation slip, κ_T/κ_S, is larger for bcc and hcp systems than for fcc systems. This suggests that the grain size effect on twinning is larger in coarse-grained bcc and hcp systems than in coarse-grained fcc systems.

Grain size effect on twinning in nc fcc materials

Deformation twinning was found to be one of the major plastic deformation mechanisms of nc fcc materials [25, 36, 56–61]. Experimentally, deformation twinning was found active in nc fcc metals even with medium to high stacking fault energy [25–27, 31, 62–64], although their coarse-grained counterparts normally do not deform by twinning. Deformation twinning was also extensively studied by molecular dynamics (MD) simulations, some of which revealed twinning as a major deformation mechanism [34], while others found twinning difficult and rare [65–68]. These reports raised a controversy on if nc fcc metals were more favorable to deformation twinning than their coarse-grained counterparts.

The above controversy was solved by the experimental observation of grain size effect on deformation twinning in nc fcc metals [40]. In a systematic study, an electrodeposited nc Ni foil with grains in the range of 10–75 nm and an average grain size of ~ 25 nm were deformed under several conditions. Very few twins were observed in the undeformed Ni sample. After the deformation, over 100 grains were examined under high-resolution electron microscopy (HREM) to check the existence of deformation twins and stacking faults. Figure 2 shows the histograms of (a) grain size distribution and (b) fractions of grains containing stacking faults and twins in samples deformed under tension at liquid nitrogen temperature at a strain rate of 3×10^{-3} s^{-1} to a strain of 5.5 %, and a flow stress of 1.5 GPa. Figure 2b shows that with decreasing grain size the fraction of grains containing twins first increases and then decreases, while the fraction of grains containing stacking faults increases monotonically. The fraction of twinned grains is a good statistical indicator of twinning propensity. Therefore, Fig. 2 indicates that with decreasing grain size the twinning propensity first increases and then decreases in nc fcc Ni. The decrease of twinning propensity with decreasing grain size is called the *inverse grain size effect* [40].

The nc Ni was also tested by split Hopkinson pressure bar (SHPB) at a strain rate of $\sim 2.6 \times 10^3$ s^{-1} at a flow stress of ~ 2 GPa, to see if similar grain size effect exists

under a different deformation condition. The result is shown in Fig. 4, which reveals a similar normal grain size effect and inverse grain size effect. In addition, comparing Fig. 4 with 3 indicates that the higher strain rate and flow stress led to larger fraction of grains that contain twins [40].

The observation of normal grain size effect and inverse grain size effect effectively reveals an optimum grain size range for the activation of deformation twinning in nc fcc metals. In other words, the deformation twinning is easiest to form at a certain grain size in the nc fcc metals. As will be demonstrated later in an analytical model [38, 39], the optimum grain size is determined by intrinsic material properties such as stacking fault energy, shear modulus, Poisson's ratio, and lattice parameter. External factors such as deformation temperature, strain rate, and applied stress may also have an effect, but this is not well understood and needs further study. The observations shown in Figs. 3 and 4 were also verified by synchrotron and neutron diffraction [69], and later observed in nc Cu [42], which has a lower stacking fault energy and very different general planar fault energies from Ni. These observations suggest that optimum grain size for twinning is a common phenomenon in nc fcc metals.

One of the salient features of the data in Figs. 3 and 4 is that no inverse grain size effect exists for stacking faults. This is believed due to the effect of generalized planar fault energies on the nucleation of twins, which makes it more difficult to activate twinning partial than to activate the first
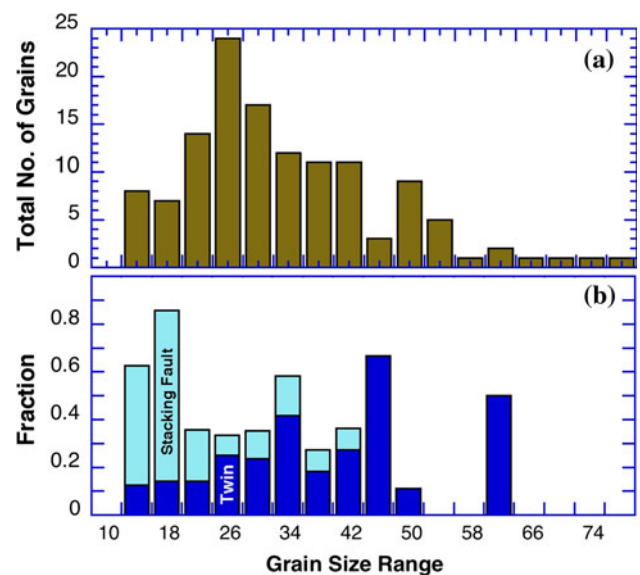

Fig. 3 Statistical grain size effect on the formations of stacking faults and deformation twins in nc Ni deformed under tension at liquid nitrogen temperature. The twin is defined as consisting of two or more layers of stacking faults on consecutive slip planes. **a** The size distribution of all grains examined under HRTEM. **b** The *fraction* distribution of grains containing stacking faults and twins [40]
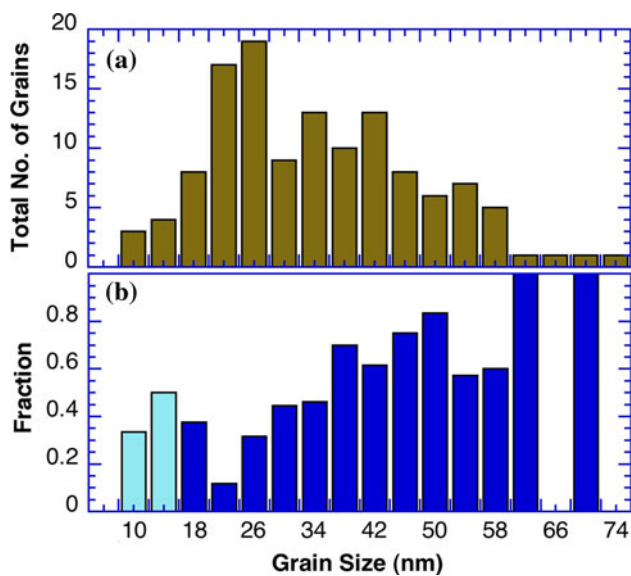
Fig. 4 Statistical grain size effect on the formations of stacking faults and deformation twins in nc Ni deformed by SHPB. **a** The size distribution of all grains examined under HRTEM. **b** The *fraction* distribution of grains containing stacking faults and twins [40]. Note that the two fraction values at the largest grain sizes are statistically insignificant

partial to form stacking fault. In other words, the observed grain size effect on the deformation twins and stacking faults can be explained by the combined effect of grain size effect and the general planar fault energy effect [40]. A recently proposed "stimulated slip" model [52] was also used to explain the inverse grain size effect on twinning [42]. However, the deformation physics assumed in the model is consistent with coarse-grained metals, not with nc metals. In addition, the "stimulated slip" model cannot explain the grain size effect on the formation of stacking faults.

Grain size effect on detwinning in nc fcc materials

Deformation-induced detwinning has been observed both experimentally [48, 50, 70–72] and in MD simulations [73]. This raises a critical issue on the effect of grain size on the competition between deformation twinning and detwinning. Understanding this issue would help us to predict the stability and evolution of microstructures and mechanical properties of nc fcc materials with twins as a major structural feature and with deformation twinning as a major deformation mechanism.

Deformation detwinning was systematically studied by Ni et al. using an electrodeposited nc Ni–20Fe (wt%) alloy with pre-existing growth twins and an average grain size of 20 nm [48]. The grain sizes were systematically increased by plastic deformation using a technique called high-

pressure torsion (HPT). Plastic deformation is known to induce grain growth in nc materials [60, 74–80]. The average grain size increased to 115 nm after 30 HPT revolutions, making it possible to study statistical changes in twin density during deformation over a wide nano-grain size range from 10 nm to over 100 nm.

Figure 5 shows the evolution of the size distribution of both all grains and the sub-set of grains containing twins with increasing numbers of HPT turns. The initial as-deposited sample has a narrow grain size distribution in the range of ~10–35 nm, and about 30 % of these grains contain growth twins that were formed during the sample synthesis (Fig. 5a). The plastic strain increases with increasing HPT turns. As shown in Fig. 5b, after 5 HPT
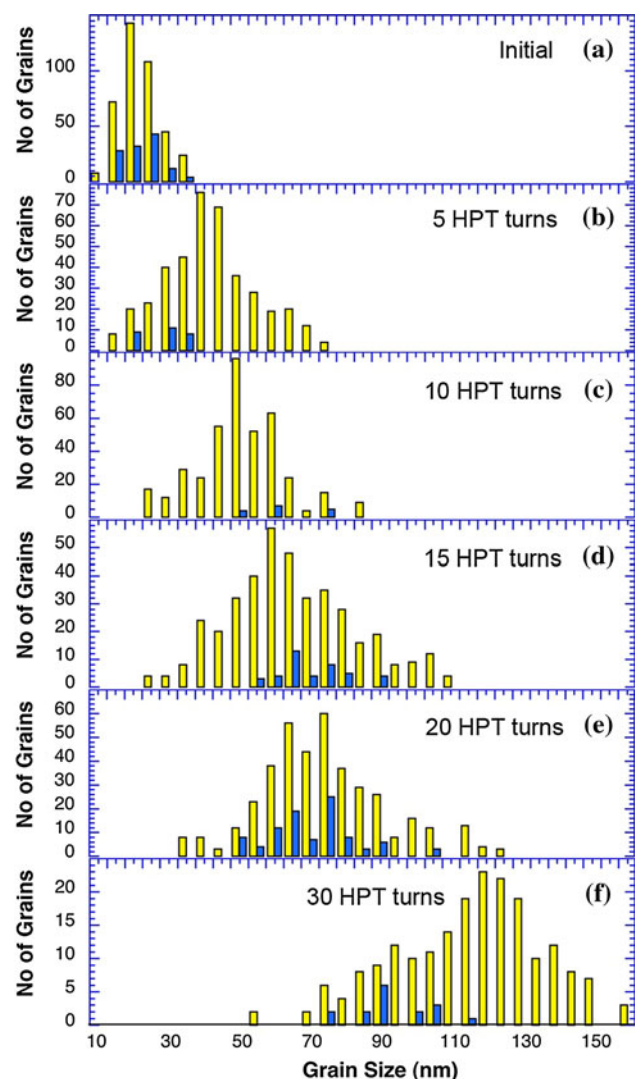

Fig. 5 The size distributions of all grains (*light yellow bars*) and grains that contain twins (*dark blue bars*) with increasing HPT turns in a nc Ni–20 wt% Fe alloy. The statistical data are measured using HRTEM, with sample in a location close to the edge of each HPT disk [48]

turns, the average grain size increased to about 40 nm and the grain size distribution was broader. Significantly, only 7 % of these grains contain twins, which is a dramatic drop from the initial state. These observations indicate that extensive detwinning occurred during the HPT deformation. Further examination of Fig. 5b–f reveals the following twinning and detwinning behavior with increasing grain sizes. At grain sizes below 40 nm, existing twins were annihilated by the detwinning process. When the grains grew to sizes above 40 nm, especially around 70 nm, twins reappeared due to the activation of deformation twinning. When grains further grew to above 110 nm, the detwinning process dominated over the twinning process, leading to the disappearance of twins.

The above experimental observations can be summarized as follows. There exists an optimum grain size range for the formation of deformation twins. Outside of this grain size range, the detwinning process dominates to annihilate existing twins. The mechanisms for these observed twinning and detwinning behavior will be discussed later in "Mechanism of detwinning in nc materials" section.

The mechanisms of the grain size effects

Mechanism of twinning transition from coarse-grains to nano-grains

The transition of twinning behavior from coarse-grained to nc fcc metals and alloys is caused by their different deformation mechanisms including dislocation sources and twinning mechanisms. Coarse-grained fcc metals are believed to twin via several conventional mechanisms including the pole mechanism [81], the prismatic glide mechanism [53], the faulted dipole mechanism [82], or other mechanisms [83–85]. These mechanisms often require a dislocation source in the grain interior to operate. The grain size effect on deformation twinning in coarse-grained metals has been explained by Fig. 2 and Table 1, using the concept of Hall–Petch type relationship. However, such relationship is empirical and the real physics based on classical dislocation theory is yet to be discovered.

Nc metals and alloys are often free of dislocations in their grain interior [57, 86], although dislocations can exist in nc grains under certain deformation conditions [13, 87]. Consequently, dislocation emission from grain boundaries becomes the primary deformation mechanisms [25–27, 34, 62, 63, 66, 67, 88–92]. Several twinning mechanisms in nc fcc metals have been reported [16, 25, 26, 31, 34, 38, 39, 41, 63, 64, 66, 67, 89, 90, 93–96], among which the most often observed is the partial emission from grain boundaries [16, 38, 39, 41, 47, 90]. As discussed in the next section, the change of deformation mechanism and

twinning mechanism also changed the effect of grain size effect on twinning, which is not surprising because different deformation mechanisms are influenced by the grain size in different ways.

Mechanism of optimum grain size for twinning in nc materials

The optimum grain size for twinning and the inverse grain size effect on twinning were predicted by an analytical model several years before the experimental observations. In the model [38, 39], the only assumption made is the emission of dislocations from grain boundaries, which was based on experimental observations and MD simulation predictions [25–27, 34, 62, 63, 66, 67, 88–92]. For simplicity, the model used a square grain cross-section (see Fig. 6). The shear stress needed for the slip of various dislocations, including the leading Shockley partial to produce a stacking faults, the twinning partial, the trailing partial, the detwinning partial, and the lattice dislocation as a function of grain size and shear stress orientation angle were calculated and compared. The dislocation that needs the lowest stress to slip is considered as the active one. A twin is considered nucleated after the leading partial generates a stacking fault across a grain and a twinning partial glides across the grain on the adjacent slip plane. For a fixed grain size, the critical shear stress that is needed to nucleate a twin is a function of shear stress orientation, and considering that grains in a nc material may be oriented in all possible directions due to their large number, the lowest shear stress to nucleate a twin at any stress orientation is considered the critical shear stress for the grain size.

Shown in Fig. 7 is the grain size effect on the critical twinning stress for nc fcc Al. The red 60° curve represents
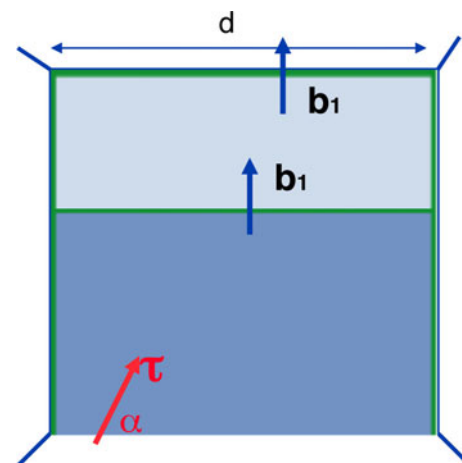

Fig. 6 A schematic illustration of a dislocation model for the nucleation of a deformation twin via the emission of a twinning partial on a (111) plane adjacent to the stacking fault plane [38, 39]
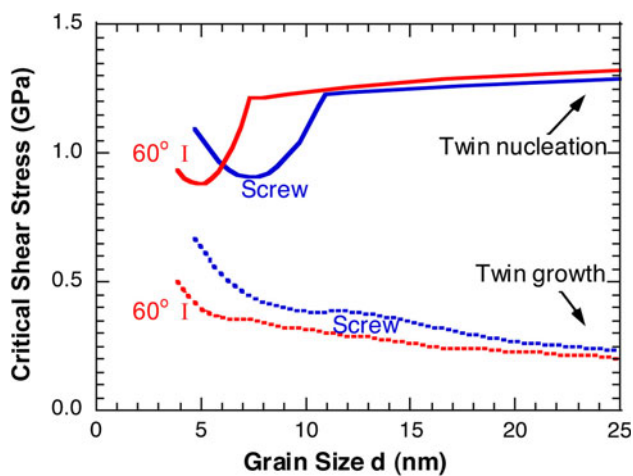
Fig. 7 A deformation map showing the critical stresses for deformation twin nucleation and growth in nc Al as a function of grain size for the 60° I and the *screw* dislocation systems [38]

Table 2 The critical stress and optimum grain size for the formation of deformation twinning in some nc fcc metals calculated using Eqs. 1 and 2 [16]

	G (GPa)	v	γ (mJ m^{-2})	A (Å)	τ_{m} (GPa)	d_{m} (nm)
Ag	30	0.37	22	4.090	0.16	73
Al	26.5	0.345	122	4.04	0.89	6
Au	27	0.44	45	4.080	0.31	30
Cu	54.6	0.343	45	3.6146	0.37	46
Ni	94.7	0.312	125	3.5232	1.06	23

the case where the 90° leading partial and 30° trailing partial form a 60° dislocation when combined, whereas the blue curve represents the case where the leading partial and trailing partial form a screw dislocation when combined. As shown, each curve has a minimum point where the critical stress for twin nucleation is lowest at an optimum grain size. In reality, most dislocations will be the mixtures of the two and their lowest twinning stresses and optimum grain sizes will be between the minimum points shown in Fig. 7. As the optimum grain size values and the critical twinning stresses for these two cases are quite close, we can define their average grain size as the optimum grain size and their average stress as the critical twinning stress, which can be approximated as [16]:

$$\tau_{\mathrm{m}} = \frac{(5.69 - 2.02v)\gamma}{2a} \tag{1}$$

and

$$\frac{d_{\mathrm{m}}}{\ln(\sqrt{2}d_{\mathrm{m}}/a)} = \frac{9.69 - v}{253.66(1 - v)} \frac{Ga^2}{\gamma}, \tag{2}$$

where τ_{m} is the critical twinning stress for a nc fcc metal, v is the Poisson's ratio, γ is the stable stacking fault energy, a is the lattice parameter, d_{m} is the optimum grain size for twinning, and G is the shear modulus. The critical stress and optimum grain size for deformation twinning in some nc fcc metals are calculated using Eqs. 1 and 2, and listed in Table 2. The predicted critical twinning stresses and optimum grain sizes agree well with experimental observations [38–40].

One of the most significant features of this model is its successful prediction of normal and inverse grain size effect on deformation twinning [40]. This is an indicator that the model indeed captured the physics of deformation twinning.

However, it also has a major deficiency: it does not consider the effect of GPFE's, which affects the nucleation and gliding of the leading and twinning partials. Consequently, this model cannot explain why no inverse grain size effect is observed for stacking faults. The physical reason for the grain size effect is the deposition of the dislocation lines on the grain boundaries as a dislocation glides under an applied stress. The deposited dislocation lines add strain energy to the system and act to drag the gliding dislocation. The dragging force does not change with grain size d, while the driving force for the dislocation slip is proportional to the length of the gliding section of the dislocation, which is grain size dependent (see Fig. 6). The driving force needs to overcome the dragging force for the dislocation to glide, and their difference in grain size dependences makes it more difficult for dislocations to move in smaller grains [16].

Mechanism of detwinning in nc materials

The detwinning could happen by the interaction between a gliding dislocation and the twin boundary. Assume the twin boundary is on the (111) plane (see Fig. 8a). If a 30° Shockley partial **Bα** glides on the $(\bar{1}1\bar{1})$ plane toward the twin boundary, it can initiate the following dislocation reaction (see Fig. 8a, [97]):

$$\mathbf{B\alpha} \rightarrow \mathbf{B\delta} + \delta\mathbf{\alpha} \tag{3}$$

The partial **Bδ** is on the (111) plane. It can slip to the left to remove one layer of the twin and produce a one-layer step at its own location. The **δα** is a stair-rod dislocation, which can dissociate under applied stress as

$$\delta\alpha \rightarrow \delta\mathbf{B} + \mathbf{B\alpha} \tag{4}$$

The partial **δB** has an opposite Burgers vector to the partial **Bδ**. It will slip to the right on the (111) plane under the same applied stress (see Fig. 8b) and create an opposing step. Such a scenario is indeed observed in the detwinning process of a nc Ni–20Fe (wt%) alloy (see Fig. 8c). When both partial **δB** and partial **Bδ** glide to the end of the twin boundary, the twin thickness will be reduced by one atomic plane. A twin could be annihilated if the above process is repeated over and over again.
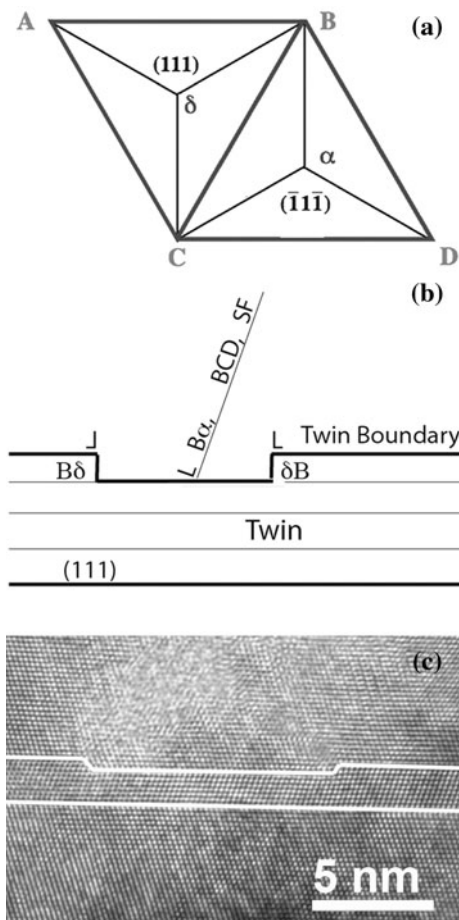
Fig. 8 a The twinning boundary plane (111) and dislocation slip plane ($\bar{1}1\bar{1}$) in the Thompson representation. **b** Illustration of a detwinning process caused by the interaction of a 30° partial dislocation L1 with the twin boundary. **c** A pair of opposing one-layer step observed in a nc Ni–20Fe (wt%) alloy, produced by the detwinning process

Another detwinning mechanism is the "stop–start three partial detwinning" mechanism reported earlier [50, 70]. Specifically, three Shockley partials with the sum of their Burgers vectors equal to 0 glide in a coordinated way to remove three twin layers. One partial glides forward first under the applied stress and stops due to a stress drop, leaving behind a stacking fault. The other two partials are then driven forward by the stacking fault and their interaction force with the first partial. A series of such set of three partials could annihilate a twin.

Optimum grain size for high twin density

Figure 5 shows an optimum grain size range in which the deformation twins appear in a large fraction of grains. This grain size range is important for designing nc fcc metals with twins as an important structural feature for enhancing the strength and ductility. For microstructures with grain

sizes outside of this range, the built-in twins will be gradually annihilated during deformation by a detwinning process. On the other hand, a stable high twin density could be maintained if the grains sizes are in this optimum range. This is a critical issue under some service conditions such as fatigue where the cyclic stress could induce extensive dislocation/twin interactions. The detwinning process could significantly soften the material, which may lead to accelerated failure.

The existence of such an optimum grain size for highest twin density can be understood with the following analysis. As discussed in "Grain size effect on twinning in nc fcc materials" and "Mechanism of optimum grain size for twinning in nc materials" sections, in a nc fcc metal there exists a grain size range within which deformation twins would form. However, the detwinning process can be caused by the interaction between the dislocation and the twin boundary, which occurs in grains of all sizes. It was found that the detwinning tendency is stronger at small grain sizes than at large grain sizes [48]. This is reasonable because the detwinning process involves dislocation interactions with twin boundaries, which needs to overcome relatively high-energy barriers [97]. Materials with smaller grains deform plastically under a higher applied stress, which makes it easier to overcome the energy barrier for detwinning. Therefore, detwinning should be statistically easier in smaller grains. From the above discussions, the tendency for twinning and detwinning during plastic deformation can be schematically illustrated as in Fig. 9. For a sample whose grain sizes are outside of the optimum grain size range, the detwinning process dominates over the twinning process, which leads to the annihilation of twins. On the other hand, for a sample whose grain sizes are in the optimum grain size range, the twinning process prevails over the detwinning process, which leads to the formation of deformation twins in a large fraction of grains. The twinning process and detwinning process eventually reached a dynamic equilibrium, which produces a stable twin density and microstructure.
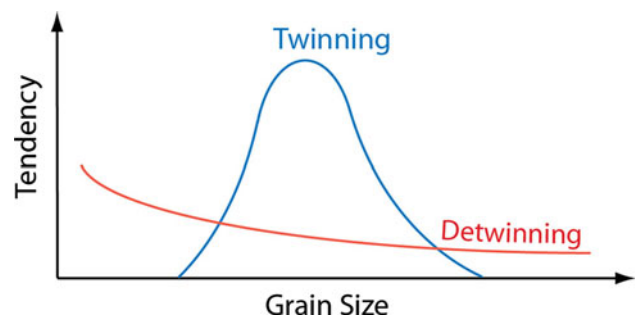

Fig. 9 Schematic representation of the grain size effect on the twinning and detwinning tendency [48]

Summary

In summary, coarse-grained fcc, bcc, and hcp metals are found more difficult to deform by twinning with decreasing grain size, whereas nc fcc metals exhibit an optimum grain size range for twinning. nc bcc and hcp metals should also have a grain size effect but this has not been studied. For nc fcc metals with grains outside of the optimum size range for twinning, plastic deformation will lead to detwinning of existing twins.

Finally, although deformation twinning does not contribute to plastic strain significantly as compared to dislocation slip, it can significantly improve the strength and ductility by blocking and accumulating dislocations at the twin boundaries, which not only strengthens the metal but also increase the strain-hardening rate. The optimum grain size for stable twinned structure is in the grain size range that is easiest for deformation twinning.

References

1. Valiev RZ, Alexandrov IV, Zhu YT, Lowe TC (2002) J Mater Res 17:5
2. Zhu YT, Liao XZ (2004) Nat Mater 3:351
3. Wang YM, Chen MW, Zhou FH, Ma E (2002) Nature 419:912
4. Horita Z, Ohashi K, Fujita T, Kaneko K, Langdon TG (2005) Adv Mater 17:1599
5. Youssef KM, Scattergood RO, Murty KL, Koch CC (2006) Scr Mater 54:251
6. Zhao YH, Liao XZ, Cheng S, Ma E, Zhu YT (2006) Adv Mater 18:2280
7. Zhao YH, Bingert JE, Liao XZ, Cui BZ, Han K, Sergueeva AV, Mukherjee AK, Valiev RZ, Langdon TG, Zhu YT (2006) Adv Mater 18:2949
8. Zhao YH, Bingert JF, Zhu YT, Liao XZ, Valiev RZ, Horita Z, Langdon TG, Zhou YZ, Lavernia EJ (2008) Appl Phys Lett 92:081903
9. Zhao YH, Zhu YT, Liao XZ, Horita Z, Langdon TG (2006) Appl Phys Lett 89:121906
10. Zhao YH, Liao XZ, Horita Z, Langdon TG, Zhu YT (2008) Mater Sci Eng A 493:123
11. Sun PL, Zhao YH, Cooley JC, Kassner ME, Horita Z, Langdon TG, Lavernia EJ, Zhu YT (2009) Mater Sci Eng A 525:83
12. Youssef K, Sakaliyska M, Bahmanpour H, Scattergood R, Koch C (2011) Acta Mater 59:5758
13. Youssef KM, Scattergood RO, Murty KL, Horton JA, Koch CC (2005) Appl Phys Lett 87:091904
14. An XH, Han WZ, Huang CX, Zhang P, Yang G, Wu SD, Zhang ZF (2008) Appl Phys Lett 92:201915
15. Christian JW, Mahajan S (1995) Prog Mater Sci 39:1
16. Zhu YT, Liao XZ, Wu XL (2012) Prog Mater Sci 57:1
17. Meyers MA, Vohringer O, Lubarda VA (2001) Acta Mater 49:4025
18. Blewitt TH, Coltman RR, Redman JK (1957) J Appl Phys 28:651
19. Li YS, Tao NR, Lu K (2008) Acta Mater 56:230
20. Meyers MA, Andrade UR, Chokshi AH (1995) Metall Mater Trans A 26:2881
21. Meyers MA, Gregori F, Kad BK, Schneider MS, Kalantar DH, Remington BA, Ravichandran G, Boehly T, Wark JS (2003) Acta Mater 51:1211
22. Cao F, Beyerlein IJ, Addessio FL, Sencer BH, Trujillo CP, Cerreta EK, Gray GT (2010) Acta Mater 58:549
23. Zhao WS, Tao NR, Guo JY, Lu QH, Lu K (2005) Scr Mater 53:745
24. Liao XZ, Srinivasan SG, Zhao YH, Baskes MI, Zhu YT, Zhou F, Lavernia EJ, Xu HF (2004) Appl Phys Lett 84:3564
25. Liao XZ, Zhao YH, Srinivasan SG, Zhu YT, Valiev RZ, Gunderov DV (2004) Appl Phys Lett 84:592
26. Liao XZ, Zhou F, Lavernia EJ, He DW, Zhu YT (2003) Appl Phys Lett 83:5062
27. Liao XZ, Zhou F, Lavernia EJ, Srinivasan SG, Baskes MI, He DW, Zhu YT (2003) Appl Phys Lett 83:632
28. Wu XL, Youssef KM, Koch CC, Mathaudhu SN, Kecskes LJ, Zhu YT (2011) Scr Mater 64:213
29. Wang ZW, Wang YB, Liao XZ, Zhao YH, Lavernia EJ, Zhu YT, Horita Z, Langdon TG (2009) Scr Mater 60:52
30. Rohatgi A, Vecchio KS, Gray GT (2001) Acta Mater 49:427
31. Chen MW, Ma E, Hemker KJ, Sheng HW, Wang YM, Cheng XM (2003) Science 300:1275
32. Zhang Y, Tao NR, Lu K (2009) Scr Mater 60:211
33. Zhao YH, Horita Z, Langdon TG, Zhu YT (2008) Mater Sci Eng A 474:342
34. Van Swygenhoven H, Derlet PM, Froseth AG (2004) Nat Mater 3:399
35. Kibey S, Liu JB, Johnson DD, Sehitoglu H (2006) Appl Phys Lett 89:191911
36. Asaro RJ, Suresh S (2005) Acta Mater 53:3369
37. Tadmor EB, Hai S (2003) J Mech Phys Solids 51:765
38. Zhu YT, Liao XZ, Srinivasan SG, Zhao YH, Baskes MI, Zhou F, Lavernia EJ (2004) Appl Phys Lett 85:5049
39. Zhu YT, Liao XZ, Srinivasan SG, Lavernia EJ (2005) J Appl Phys 98:034319
40. Wu XL, Zhu YT (2008) Phys Rev Lett 101:025503
41. Zhu YT, Liao XZ, Wu XL (2008) JOM 60(9):60
42. Zhang JY, Liu G, Wang RH, Li J, Sun J, Ma E (2010) Phys Rev B 81:172104
43. Liao XZ, Zhao YH, Zhu YT, Valiev RZ, Gunderov DV (2004) J Appl Phys 96:636
44. Gu P, Dao M, Asaro RJ, Suresh S (2011) Acta Mater 59:6861
45. Dobron P, Chmelik F, Yi SB, Parfenenko K, Letzig D, Bohlen J (2011) Scr Mater 65:424
46. Gu P, Kad BK, Dao M (2010) Scr Mater 62:361
47. Asaro RJ, Krysl P, Kad B (2003) Philos Mag Lett 83:733
48. Ni S, Wang YB, Liao XZ, Li HQ, Figueiredo RB, Ringer SP, Langdon TG, Zhu YT (2011) Phys Rev B 84:235401
49. Shute CJ, Myers BD, Liao Y, Li SY, Hodge AM, Barbee TW, Zhu YT, Weertman JR (2011) Scr Mater 65:899
50. Wang J, Li N, Anderoglu O, Zhang X, Misra A, Huang JY, Hirth JP (2010) Acta Mater 58:2262
51. Fu HH, Benson DJ, Meyers MA (2001) Acta Mater 49:2567
52. Yu Q, Shan ZW, Li J, Huang XX, Xiao L, Sun J, Ma E (2010) Nature 463:335
53. Venables JA (1961) Philos Mag 6:379
54. Hirth JP, Lothe J (1992) Theory of dislocations. Krieger Publishing Company, Malabar, FL, p 811
55. Liao XZ, Huang JY, Zhu YT, Zhou F, Lavernia EJ (2003) Philos Mag 83:3065
56. Schiotz J, Di Tolla FD, Jacobsen KW (1998) Nature 391:561
57. Shan ZW, Stach EA, Wiezorek JMK, Knapp JA, Follstaedt DM, Mao SX (2004) Science 305:654

58. Van Swygenhoven H, Derlet PM, Hasnaoui A (2002) Phys Rev B 66:024101
59. Kumar KS, Suresh S, Chisholm MF, Horton JA, Wang P (2003) Acta Mater 51:387
60. Liao XZ, Kilmametov AR, Valiev RZ, Gao HS, Li XD, Mukherjee AK, Bingert JF, Zhu YT (2006) Appl Phys Lett 88:021909
61. Rice JR (1992) J Mech Phys Solids 40:239
62. Wu X, Zhu YT, Chen MW, Ma E (2006) Scr Mater 54:1685
63. Wu XL, Liao XZ, Srinivasan SG, Zhou F, Lavernia EJ, Valiev RZ, Zhu YT (2008) Phys Rev Lett 100:095701
64. Zhu YT, Liao XZ, Valiev RZ (2005) Appl Phys Lett 86:103112
65. Yamakov V, Wolf D, Phillpot SR, Gleiter H (2002) Acta Mater 50:5005
66. Yamakov V, Wolf D, Phillpot SR, Mukherjee AK, Gleiter H (2002) Nat Mater 1:45
67. Yamakov V, Wolf D, Phillpot SR, Mukherjee AK, Gleiter H (2004) Nat Mater 3:43
68. Wolf D, Yamakov V, Phillpot SR, Mukherjee A, Gleiter H (2005) Acta Mater 53:1
69. Cheng S, Stoica AD, Wang XL, Ren Y, Almer J, Horton JA, Liu CT, Clausen B, Brown DW, Liaw PK, Zuo L (2009) Phys Rev Lett 103:035502
70. Li N, Wang J, Huang JY, Misra A, Zhang X (2011) Scr Mater 64:149
71. Li L, Ungar T, Wang YD, Morris JR, Tichy G, Lendvai J, Yang YL, Ren Y, Choo H, Liaw PK (2009) Acta Mater 57:4988
72. Wen HM, Zhao YH, Li Y, Ertorer O, Nesterov KM, Islamgaliev RK, Valiev RZ, Lavernia EJ (2010) Philos Mag 90:4541
73. Yamakov V, Wolf D, Phillpot SR, Gleiter H (2003) Acta Mater 51:4135
74. Zhang K, Weertman JR, Eastman JA (2004) Appl Phys Lett 85:5197
75. Zhang K, Weertman JR, Eastman JA (2005) Appl Phys Lett 87:061921
76. Jin M, Minor AM, Stach EA, Morris JW (2004) Acta Mater 52:5381
77. Wang YB, Li BQ, Sui ML, Mao SX (2008) Appl Phys Lett 92:011903
78. Sansoz F, Dupont V (2006) Appl Phys Lett 89:111901
79. Fan GJ, Wang YD, Fu LF, Choo H, Liaw PK, Ren Y, Browning ND (2006) Appl Phys Lett 88:171914
80. Wang YB, Ho JC, Liao XZ, Li HQ, Ringer SP, Zhu YT (2009) Appl Phys Lett 94:011908
81. Ookawa AJ (1957) Phys Soc Jpn 12:825
82. Niewczas M, Saada G (2002) Philos Mag A 82:167
83. Mahajan S, Chin GY (1973) Acta Metall 21:1353
84. Mahajan S, Green ML, Brasen D (1977) Metall Trans A 8:283
85. Thompson N (1953) Proc Phys Soc Lond Sect B 66:481
86. Zhu YT, Huang JY, Gubicza J, Ungar T, Wang YM, Ma E, Valiev RZ (2003) J Mater Res 18:1908
87. Wu XL, Zhu YT, Wei YG, Wei Q (2009) Phys Rev Lett 103:205504
88. Wu XL, Qi Y, Zhu YT (2007) Appl Phys Lett 90:221911
89. Wu XL, Zhu YT (2006) Appl Phys Lett 89:031922
90. Zhu YT, Wu XL, Liao XZ, Narayan J, Mathaudhu SN, Kecskes LJ (2009) Appl Phys Lett 95:031909
91. Derlet PM, Van Swygenhoven H, Hasnaoui A (2003) Philos Mag 83:3569
92. Van Swygenhoven H (2002) Science 296:66
93. Narayan J, Zhu YT (2008) Appl Phys Lett 92:151908
94. Wu XL, Narayan J, Zhu YT (2008) Appl Phys Lett 93:031910
95. Zhu YT, Narayan J, Hirth JP, Mahajan S, Wu XL, Liao XZ (2009) Acta Mater 57:3763
96. Li BQ, Li B, Wang YB, Sui ML, Ma E (2011) Scr Mater 64:852
97. Zhu YT, Wu XL, Liao XZ, Narayan J, Kecskes LJ, Mathaudhu SN (2011) Acta Mater 59:812